Polymer Chemistry

ROYAL SOCIETY
OF CHEMISTRY

PAPER

CrossMark
← click for updates

Synthesis of non-fouling poly[*N*-(2-hydroxypropyl)-methacrylamide] brushes by photoinduced SET-LRP†

Mariia Vorobii,[a] Andres de los Santos Pereira,[a] Ognen Pop-Georgievski,[a] Nina Yu. Kostina,[a] Cesar Rodriguez-Emmenegger*[a,b] and Virgil Percec*[b]

Surface-initiated photoinduced single-electron transfer living radical polymerization (SET-LRP) was employed to assemble brushes of poly[*N*-(2-hydroxypropyl) methacrylamide] (poly(HPMA)) from silicon surfaces. The linear increase in thickness of the poly(HPMA) brushes with time and the ability to prepare block copolymers indicate the living nature of this grafting-from process. Copper concentrations as low as 80 ppb were sufficient for this surface-initiated SET-LRP. Micropatterns of poly(HPMA) brushes on the silicon surface were constructed for the first time by this method. Negligible fouling was observed after contact with undiluted blood plasma. This report provides the first example of non-fouling polymer brushes prepared by SET-LRP of HPMA.

Introduction

The development of surface-initiated living radical polymerization techniques to prepare non-fouling polymer brushes with complex architectures is fundamental for improving the performance of biomaterials that interface with biological media or tissues, as well as to confer specific functions to surfaces. The ability to tailor the interactions between artificial surfaces and biological systems is of the utmost importance for the success of devices operating in direct contact with a biological environment.[1,2] Among the interactions to be tailored, the prevention of non-specific interactions commonly referred to as fouling typically mediated by the rapid adsorption of biomolecules is especially important. Protein fouling from complex biological fluids, particularly blood, plasma, and serum, is a ubiquitous and adverse event that impairs the properties and functions of various biotechnological and biomedical devices.[3–6] Some examples include stopping flow through separation columns and porous membranes,[7] non-specific response of affinity biosensors,[4,5,8] reduced circulation time of nanocarriers in the bloodstream due to colloidal instability[9] or opsonization,[10–14] bacterial attachment on contact lenses[15] and synthetic grafts,[16] or disabling of cardio-

vascular devices by thrombus formation.[2] Remarkably, protein fouling controls the way in which cells and tissues interact with implants and the foreign body responses, and ultimately dictates the biocompatibility of the material.[17]

A promising approach to design bioactive surfaces involves the immobilization of biomolecules or bioreceptors able to perform the desired function onto an ultra-thin film coating the material surface. The function of this coating is to prevent protein fouling. The rationale behind the design of surfaces capable of preventing fouling, hereafter termed *non-fouling*, is based on the minimization of the forces which drive proteins to bind to surfaces, namely the hydrophobic effect, Coulombic interactions, and hydrogen bonding.[18] Various types of surface modifications reducing fouling (that is, *antifouling*) have been developed based on self-assembled monolayers (SAMs),[19] grafted polymer layers, and "grafted-from" polymer brushes.[2] Most of these surface modifications resulted in a full prevention of the fouling from the main plasma proteins, human serum albumin (HSA) and fibrinogen (Fbg), as well as from immunoglobulin G (IgG). However, only brushes based on oligo(ethylene) methacrylates (MeOEGMA), hydroxyethyl methacrylate and hydroxyethyl acrylamide provided fouling levels below 300 pg mm^{-2} (about 10% of a protein monolayer) when challenged with real biological fluids instead of simple model solutions.[20–22] Zwitterionic polymer brushes of phosphorylcholine methacrylate, sulfobetaine methacrylate and various carboxybetaines were introduced based on the assumption that hydration posed the most important barrier to protein fouling.[23,24] However, only poly(carboxybetaine acrylamide) brushes resulted in full resistance to blood plasma.[21,25] Recently a second polymer brush that showed

[a]*Institute of Macromolecular Chemistry, Academy of Sciences of the Czech Republic, v.v.i., Heyrovsky sq. 2, 162 06 Prague, Czech Republic. E-mail: rodriguez@imc.cas.cz*
[b]*Roy & Diana Vagelos Laboratories, Department of Chemistry, University of Pennsylvania, Philadelphia, Pennsylvania 19104-6323, USA. E-mail: percec@sas.upenn.edu*

non-fouling properties, based on poly[N-(2-hydroxypropyl) methacrylamide] (HPMA) was introduced by one of our laboratories.[26] Poly(HPMA) was introduced in 1973 by Kopeček laboratory to become one of the most successful polymers employed in drug delivery vehicles.[27–29] Since its first synthesis, poly(HPMA) has been extensively studied for use in polymer-drug conjugates or copolymerized to form drug- and gene-delivery vehicles or nanoparticles to carry drugs, among other applications.[29–31] Brushes of poly(HPMA) were shown to resist fouling from undiluted human plasma or serum, as well as calf serum, for 15 min.[26] This non-fouling behavior was also observed for five other undiluted human or animal biofluids: human cerebrospinal fluid, saliva, and urine, as well as chicken egg and whole cow milk.[20] More extensive contact with blood plasma for up to 10 h or even with whole blood and its components did not lead to fouling on the surface.[32]

The preparation of poly(HPMA) brushes relied on surface-initiated atom transfer radical polymerization (ATRP).[26] However, ATRP in bulk or solution of HPMA (1-butanol, DMF) as well as for other (meth)acrylamides resulted in low monomer conversion (19% in 23 h) and did not proceed by a living process.[33–35] Similarly, the surface-initiated ATRP does not proceed by a living process, cannot be re-initiated and after few minutes no further growth is observed.[26] The livingness of the polymerization as well as the ability to finely tune the thickness of the brush are not only desirable but are absolutely necessary in order to access more complex surface architectures, as required for bioactive surfaces. For instance, the activation of the functional groups on side chains along the whole thickness of antifouling polymer brushes is known to impair their resistance to fouling.[36] More versatile strategies based on chain-end functional group activation and the use of click chemistry ligations compatible with the biological molecules and applications show great promise to overcome this issue,[37] as they would result in minimal changes to the fouling resistance. However, such strategies have not yet been applied to polymer brushes based on HPMA or other methacrylamides grown by any metal-catalyzed polymerization as no halogen end-groups remain after the process. Additionally, the lack of livingness prevents the attainment of multiblock copolymers featuring other functions in addition to the resistance to fouling critically reducing the synthetic toolkit and the complex functions a surface could have. The reversible addition fragmentation transfer (RAFT) polymerization of HPMA in a range of polar solvents (water, DMSO, DMF) has been used extensively to prepared narrowly dispersed poly(HPMA) with various chain end functionalities while allowing to achieve almost quantitative monomer conversion as well as preparation of block copolymers.[29,38,39] The RAFT process could in principle be carried out from the surface by immobilizing the chain transfer agent via its R-group.[40] The deactivation mechanism relies on the transfer of the radical to a polymer capped with chain-transfer agent which is in solution. The latter process is restricted by the diffusion of large polymers to the surface resulting in thickness and grafting densities which are lower than the ones obtained by ATRP, thereby limiting the applicability of surface RAFT polymerization for non-fouling surfaces.[41]

An alternative to ATRP is the single electron transfer living radical polymerization (SET-LRP).[42–46] In contrast to ATRP, SET-LRP uses very low amounts of Cu^0 to generate radicals from alkyl halides, has a remarkably high living nature,[47,48] perfect or near perfect polymer chain-end-group functionality,[48,49] and is capable to polymerize a broad range of monomers in various polar solvent solvents including water.[47,50–56] By comparison with other metal-catalyzed polymerizations, SET-LRP achieves fast reaction rates and can provide quantitative monomer conversion, 100% chain end functionality[48] and very high molecular weights,[46] due to near-complete suppression of termination reactions.[47,48,53–55,57] In particular, while the ATRP of HPMA using 2-methyl chloropropionate (MCP)/CuCl/Me_6TREN in ethanol reached low conversion (19% in 23 h),[58] SET-LRP of the same monomer in water using MCP/Cu wire/ Me_6TREN afforded 90% monomer conversion after 15 h.[52] Recently a photoinduced variant of SET-LRP has been introduced.[59] This process is mediated by $CuBr_2$ in the presence of an excess of an aliphatic tertiary amine, usually Me_6TREN, and provides excellent living characteristics.[59] The photoinduced SET-LRP exploits the outer-sphere single electron transfer from the photo-excited tertiary amine to an alkyl halide initiator, resulting in heterolysis of the C–X bond. This provides the initiating radical, while the deactivation is mediated by $Cu(Me_6TREN)X_2$, which was regenerated by the disproportionation of $Cu(Me_6TREN)X$.[59] Photoinduced SET-LRP was subsequently utilized to graft methyl acrylate and diethyleneglycol acrylate from cellulose.[60]

Here we report the grafting of up to 220 nm thick brushes of poly(HPMA) from a self-assembled monolayer (SAM) of initiator on a silicon surface by photoinduced SET-LRP of HPMA. The polymerization proceeded very fast, even when very low concentrations of Cu (0.08 to 8.0 ppm) were employed. The evolution of polymer brush thickness with irradiation time in the absence of sacrificial initiator was followed by ellipsometry and was found to increase linearly even at very low catalyst concentrations enabling to precisely access thickness ranging from few to 220 nm. The living character of the process was established by carrying out the reinitiation of the same monomer by SET-LRP from the brush as well as by the preparation of diblock copolymer brushes. The use of light as a trigger for the SET-LRP allowed the creation of micropatterned surfaces of poly(HPMA) brushes. The excellent resistance of these brushes to fouling from blood plasma was demonstrated using surface plasmon resonance. It is envisioned that this method will further expand the synthetic toolbox for the design and creation of antifouling bioactive interfaces for biomaterials.

Results and discussion

Photoinduced grafting-from of polymer brushes

Poly(HPMA) brushes with a thickness up to 220 nm were grown via photoinduced SET-LRP from initiators grafted to
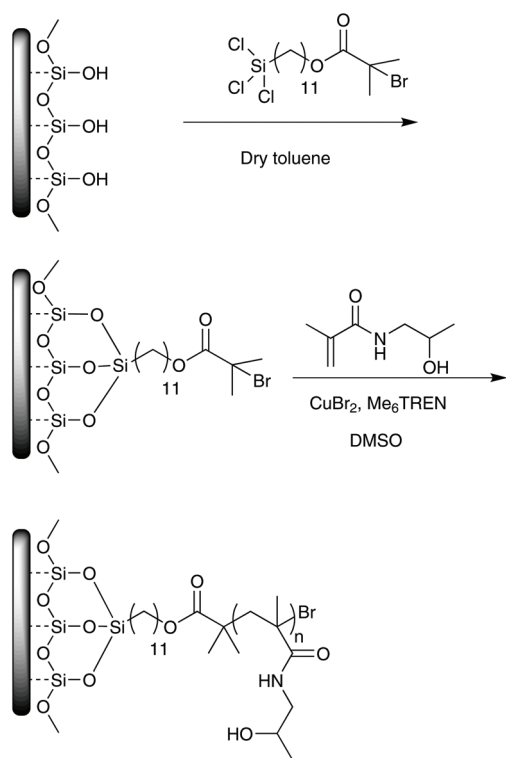
planar surfaces. The initiator, 11-(trichlorosilyl)undecyl 2-bromo-2-methylpropanoate, was assembled on freshly activated silicon substrates (Scheme 1). From the range of molecules known to self-assemble on silicon, a trichlorosilane featuring an undecyl spacer was selected as initiator. Other initiators based on trialkoxysilanes or chlorodialkylsilanes have led to ill-defined SAMs with the concomitant detachment of large areas during the polymerization as a result of the osmotic pressure exerted by the growing brushes in thermodynamically good solvents.[61–63]

The successful grafting of the self-assembled monolayer (SAM) of initiator was evidenced by AFM, ellipsometry, XPS and GAATR-FTIR spectroscopy. AFM topographic images (tapping mode in air, see ESI†) revealed that the SAM of initiator was homogeneous, without pinholes and featuring a roughness, R_q = 1.2 nm. The XPS spectrum of the C 1s region of the initiator SAM (Fig. 1a) shows a marked predominance of the C–C, C–H component at 285.0 eV, attributed to the alkane backbone of the initiator SAM. Moreover, the envelopes corresponding to the C–Si bond and the ester group and tertiary carbon of the initiator head group are also resolved. The presence of Br chain ends is also confirmed by the high resolution Br 3d spectrum. The Br 3d envelope could be deconvoluted with one spin–orbit splitting doublet with contributions at 70.6 eV (Br $3d_{5/2}$) and 71.6 eV (Br $3d_{3/2}$). Additional evidence of the chemical structure of the SAM was obtained from the GAATR-FTIR spectrum (Fig. 1b). The alkyl chain of the initiator is confirmed by an intense band at 2925 cm^{-1} and another at 2854 cm^{-1} stemming from the asymmetric and symmetric C–H stretching vibrations. The ester group is evidenced by the presence of peaks at 1738 cm^{-1} (C–O stretch), 1238 cm^{-1} (asymmetric C–O–C stretch), 1167 cm^{-1} (symmetric C–O–C stretch), and at 1113 cm^{-1} (asymmetric C–O stretch). The formation of the SAM led to an increase in thickness of 0.97 ± 0.04 nm as determined by ellipsometry. Dynamic water contact angle revealed a drastic change in the wettability of the surface (θ_{adv} = 82° and θ_{rec} = 72°) reflecting the more hydrophobic nature of the initiator compared to the fully wettable freshly plasma-cleaned silicon wafers. The SAM was exploited as the initiating site for the grafting of poly(HPMA) brushes *via* photoinduced SET-LRP. Poly(HPMA) brushes of up to 220 nm could be grown in less than 60 min. The chemical structure of the obtained poly(HPMA) brushes was confirmed by XPS and GAATR-FTIR measurements. The C 1s region of the spectrum shows the presence of the amide bond at 288.1 eV, as well as a predominance of the C–C, C–H peak (Fig. 1, a). The presence of components for C–O, C–N and tertiary carbon with areas in a ratio of close to 1 : 1 : 1 corresponds well with the expected structure. Further proof of the chemical structure of poly(HPMA) brushes can be obtained from the N 1s and O 1s high resolution XPS spectra (Fig. 1, d and e). A single peak at 400 eV in the N 1s spectrum arises from the amide nitrogen, while two peaks at 532.8 and 531.6 eV arising from C=O and C–O bonds are visible in the O 1s spectrum. The presence of prominent peaks at 1637 and 1529 cm^{-1} in the GAATR-FTIR spectrum (Fig. 1, b) corresponding to the amide I and II bands respectively further confirms the chemical structure of the brushes. The broad absorption at 3345 cm^{-1} is characteristic of the H-bonded hydroxyl group. Importantly, the survey spectrum (Supporting Fig. SF3 in the ESI†) shows no residual copper after the polymerization, which is a desired advantage for various bioapplications.

The surface thickness was highly homogeneous on the surface of all samples as evidenced by the low standard deviation the ellipsometric thickness, usually less than of 2 nm. The topography of the surfaces was accessed by AFM in tapping mode. Fig. 1f depicts the topographic image of a 30 nm-thick poly(HPMA) brush prepared in DMSO/water using 80 ppb of Cu. Even using such low concentrations of catalyst, very homogeneous surfaces were obtained as characterized by the mean square roughness R_q of 1.32 ± 0.27 nm, close to the initiator SAM. The homogeneity of the surface and lack of any pinholes suggest uniform initiation on the surface.

As expected, the grafting of poly(HPMA) brushes caused a pronounced increase in the wettability of the surface (θ_{adv} = 35° and θ_{rec} = 9°). The large increase in the wettability is of fundamental importance when biological applications of the surfaces are to be targeted. Hydrophobic surfaces promote protein fouling mediated by the hydrophobic effect, which leads to a series of detrimental effects for most applications.[18,64,65]

Scheme 1 Surface-initiated photoinduced SET-LRP of HPMA from bromoisobutyrate-functionalized self-assembled monolayer on silicon.
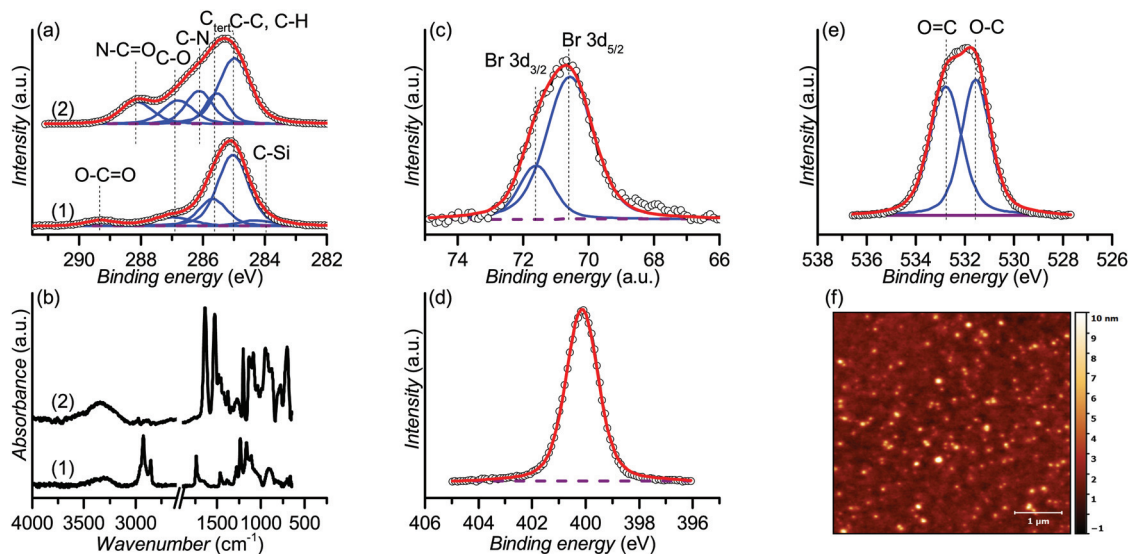
Fig. 1 (a) High-resolution XPS spectra of the C 1s region and (b) GAATR-FTIR spectra of the SAM of initiator (1) and 30 nm-thick poly(HPMA) brush (2). (c) High resolution XPS spectrum Br3d region of initiator, (d) and (e) high resolution XPS spectra of the N 1s and O 1s region of poly(HPMA) brushes. (f) Representative topography image of 30 nm-thick poly(HPMA) brushes obtained by AFM in tapping mode. $[HPMA]_0 = 1.76$ M, $[CuBr_2]_0 = 1.66$ μM (80 ppb), $[Me_6TREN]_0 = 9.96$ μM, DMSO/water 1:1.

Kinetic studies of photoinduced SET-LRP of HPMA

As in the case of other surface-confined polymerizations the monomer conversion is negligible (less than 0.01%) and the mass of the polymer at the surface is in the range of ng and therefore too small for size exclusion chromatography analysis. As an example for the thickest poly(HPMA) brushes (250 nm) grown in an area of 1 cm^2 the mass of the polymer can be estimated to be approximately 250 ng. This mass represents a monomer conversion of about 0.002%. Therefore, the evolution of the brush thickness in time was utilized to assess the kinetics of surface-initiated SET-LRP. Kinetic studies were conducted to confirm the livingness of the photoinduced SET-LRP (Fig. 2). The polymerization was carried out in either pure DMSO or DMSO/water with two concentrations of CuBr$_2$ (8.0 ppm and 80 ppb). The lowest concentration of copper employed here is below the usual concentration utilized for Initiators for Continuous Activator Regeneration (ICAR) ATRP minimizing the risk of residual copper on the surface potentially toxic for cells.[66] A generally linear evolution of the thickness with time was observed for all the conditions during the 60 min polymerization, indicating pseudo-first order kinetics. Lower concentrations of Cu led to slightly faster growth and a constant rate during the studied time period. The choice of solvent caused a more pronounced effect on the rate of polymerization. The introduction of water led to an approximately 5-fold increase in the rate of polymerization as well as in the final thickness achieved. It is noteworthy that brushes of up to 220 nm could be prepared in just 60 min of polymerization. Excluding either irradiation, initiator, or the catalyst from the reaction system prevented any grafting of poly(HPMA)
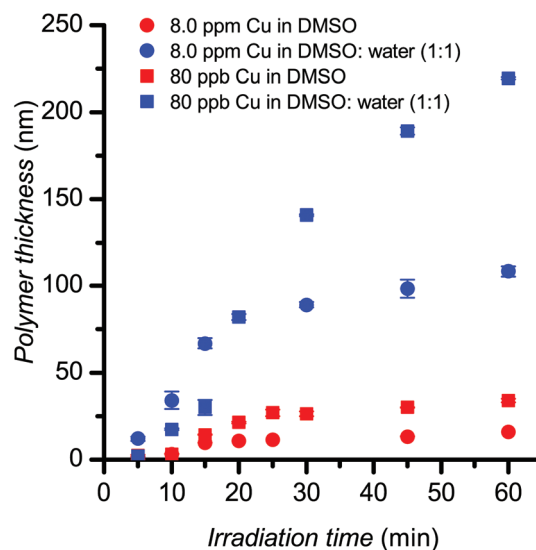

Fig. 2 Polymer thickness of dry poly(HPMA) brushes as a function of polymerization time. Polymerization conditions $[HPMA]_0 = 1.76$ M, solvent DMSO (red) or DMSO/water 1:1 (blue). Catalyst concentration: $[CuBr_2]_0 = 166$ μM (8 ppm, circles) or $[CuBr_2]_0 = 1.66$ μM (80 ppb, squares). $[Me_6TREN]_0 = 6 \times [CuBr_2]$. The markers represent the mean values and the error bars show the standard deviation of the thickness of three points.

(for control experiments Supporting Table ST2 in the ESI†) evidencing that the polymerization followed a photoinduced mechanism and was confined to the silicon surface.

Assessment of the livingness of photoinduced SET-LRP of HPMA

The constant rate of growth of the brushes is a good indication of the successful photoinduced SET-LRP of HPMA. However, the light-triggered initiation of the polymerization and linear growth may not be sufficient to imply the livingness of the polymerization.[48] Therefore further proof of the end-group fidelity is necessary in order to establish the living character of the process.[48] The ability to re-initiate the polymerization from the chain end of the poly(HPMA) brushes is a direct proof of the fidelity of the end-groups and thus evidences the livingness of the system.[48,57,67] Experiments were performed in which the polymerizations were stopped and resumed (Fig. 3). Re-initiation, and resumed growth of the polymer brush, is only possible if the brushes bear the Br end-group. Poly(HPMA) brushes 20 nm-thick were prepared in DMSO/water using 80 ppb of Cu. After characterization of the brushes the polymerization was resumed to yield poly(HPMA) brushes with an overall thickness of 170 nm. Remarkably, the thickness of the re-initiated brush is close to the thickness of brushes prepared by a continuous polymerization for the same irradiation time (Fig. 3). This underpins that the re-initiated polymerization proceeded at the same rate as the polymerization with continuous irradiation, and suggests that a high proportion of the chains were end-capped with Br and thus bimolecular termination was minimal. This is in close agreement with recent reports showing that SET-LRP gives access to close to quantitative chain end functionalities for a Cu-catalyzed polymerization.[47,48,57]
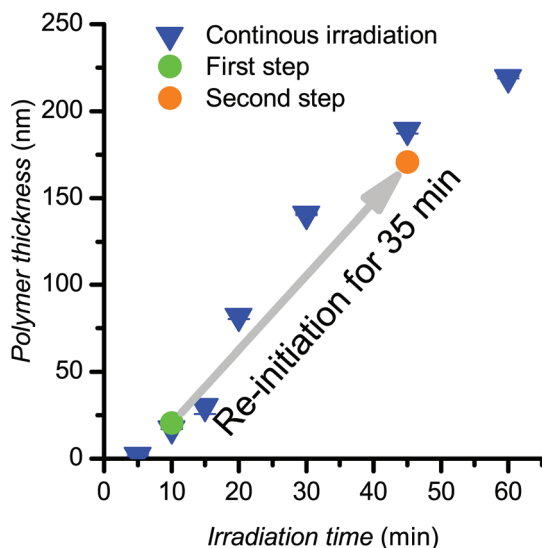

Fig. 3 Dry ellipsometric thickness of a re-initiated polymerization carried out in DMSO/water (1 : 1) with 80 ppb Cu. Initial irradiation for 10 min yielded poly(HPMA) brushes of thickness 20.5 ± 0.3 nm (green). The brushes were utilized as macroinitiators for a subsequent polymerization (for an additional 35 min) to yield poly(HPMA) brushes of thickness 170.7 ± 0.8 nm (red). The kinetics with continuous irradiation is shown for comparison in blue.

The ability to design complex surface architectures gives access to a larger number of routes to tailor the properties of a surface and the functions which the surface can perform. Even the preparation of simple diblock copolymers has the livingness of the polymerization as a prerequisite. To illustrate this, MeOEGMA was grafted from poly(HPMA) brushes. The macro-initiators, poly(HPMA) brushes, were prepared in DMSO/water using 80 ppb of Cu to yield brushes of length 54.2 ± 3.0 nm. In a subsequent step MeOEGMA was polymerized by photo-induced SET-LRP in pure DMSO, using 8.0 ppm of Cu. A total thickness of 188.2 ± 1.3 nm was measured for the diblock polymer brushes, corresponding to a thickness increase of 130 nm as a consequence of the growth of the second polymer block.

The change in the chemical structure of the layer was evidenced by GAATR-FTIR, confirming the presence of the features typical of both polymer blocks (Supporting Fig. SF4 in the ESI†). Furthermore, depth profiling of the chemical structure was performed by XPS by acquiring spectra after increasing times of etching with Ar gas clusters. Fig. 4a depicts the evolution of the C 1s region of the XPS spectrum of poly(HPMA-b-MeOEGMA) with increasing etch depth. The uppermost layer of the brush shows a clear predominance of the C–O peak at 286.6 eV.

The presence of this peak corresponds well to the chemical structure of poly(MeOEGMA) and its oligo(ethylene glycol) side chains. Interestingly, the intensity observed for the C–O peak markedly decreases with increasing the etch depth. At the same time, an increase is observed for the C–C, C–H, C–N, and O=C–N components, in line with an enrichment of the composition in poly(HPMA). Effectively, the formation of the diblock copolymer brush leads to a gradual change in the contributions of the C–O, C–C, C–H, C–N, and O=C–N moieties, due to the back-coiling of the polymer chains (Fig. 4b). Nevertheless, the preferential localization of the poly(HPMA) block close to the substrate and poly(MeOEGMA) block far from the substrate can be clearly visualized by the distinct C 1s XPS spectra measured along the z-axis. The XPS data confirm the chain extension of poly(HPMA) by MeOEGMA. The grafting of a poly(MeOEGMA) block also led to an increase in the water contact angles (θ_{adv} = 67° and θ_{rec} = 17°).

To the best of our knowledge, no metal-catalyzed radical polymerization has been described that provides living features for the surface polymerization of methacrylamides even using high concentrations of catalysts. While various thicknesses have been achieved, neither living features, nor a constant evolution of the thickness of the brush with time, was observed.[26]

The attainment of the diblock architecture using photo-induced SET-LRP is a direct proof of the preservation of the polymer-growing centers and evidences the living character of the process. The latter observation, together with the very high rate, high and readily tunable thicknesses for a methacrylamide compared to other metal-catalyzed surface-initiated radical polymerizations, underpins the advantages of the SET-LRP for the polymerization of methacrylamide monomers
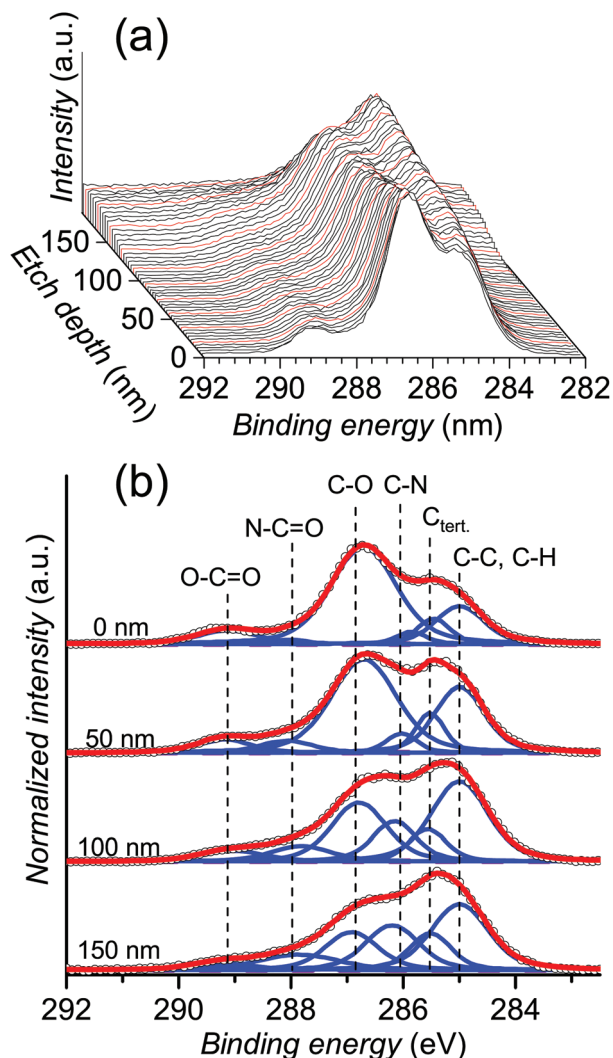
Fig. 4 XPS depth profile of poly(HPMA-*b*-MeOEGMA). (a) Evolution of the C 1s XPS spectrum with etch depth. (b) Comparison of normalized the C 1s XPS spectra at four etch depths. The total thickness of the poly (HPMA-*b*-MeOEGMA) was 188.2 ± 1.8 nm and of the first block of poly (HPMA) was 54.2 ± 3.0 nm.
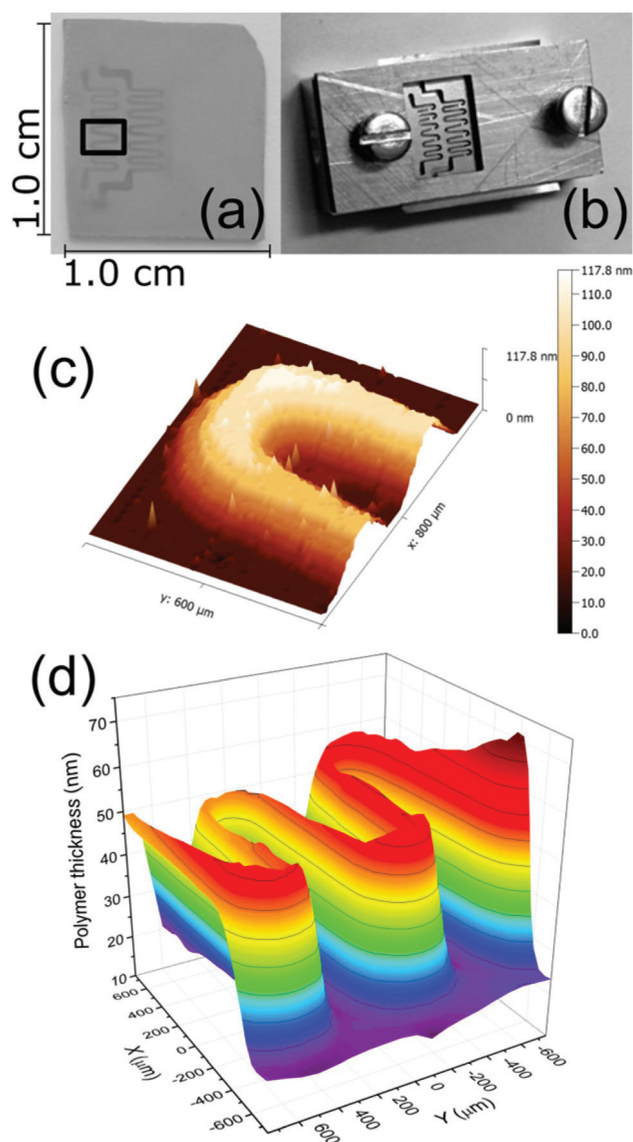

Fig. 5 Patterning of poly(HPMA) brushes using photoinduced SET-LRP. (a) Optical image of the pattern, (b) picture of the sample holder featuring the shadow mask used, (c) profilometry of a small area of the pattern and (C) ellipsometric mapping of the pattern. [HPMA] = 1.76 M, [CuBr$_2$] = 1.66 μM (80 ppb), [Me$_6$TREN] = 9.96 μM, DMSO/water 1 : 1.

and is in line with our previous results on the polymerization of HPMA in solution.[52]

Patterning of poly(HPMA) brushes

The patterning of surfaces induced by light results in advantages over more widely used methods such as μ-contact printing, which is marred by problems due to deformation of the stamp and diffusion of the ink, for example.[68] Selective irradiation of an SAM of initiator was expected to restrict polymerization to those regions under irradiation. Indeed, confining the irradiation to precise regions using a shadow mask (Fig. 5b) enabled the selective growth of poly(HPMA) brushes exclusively from irradiated areas. After 30 min of polymerization of HPMA (in DMSO : water using 80 ppb of Cu), a patterned surface visible to the naked eye was generated

(Fig. 5a). Stylus profilometry (Fig. 5c) and ellipsometric mapping (Fig. 5d) confirmed the successful pattern of the surface. The small size of the stylus head of the profilometer accounted for a comparatively more precise mapping than ellipsometry. The sharp pattern observed by profilometry highlights the power of photoinduced SET-LRP to prepare microengineered surfaces.

Resistance to protein adsorption

The resistance to protein fouling of the prepared brushes of poly(HPMA) was studied by surface plasmon resonance (SPR). An SAM of ω-mercaptoundecyl bromoisobutyrate was prepared
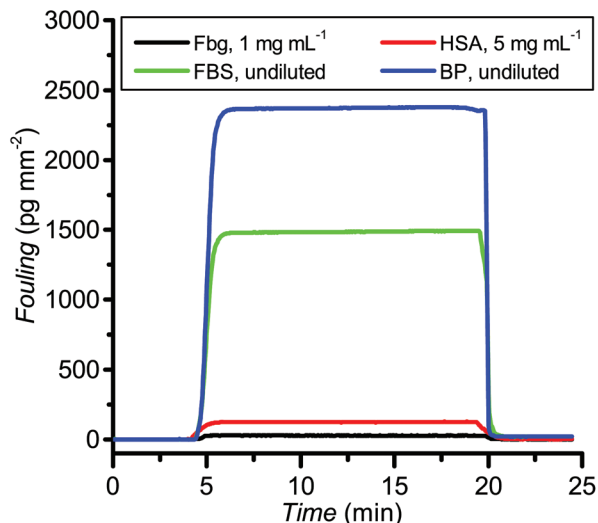
Fig. 6 Protein fouling on poly(HPMA) brushes (40 nm) as characterized by SPR. Black: fibrinogen (Fbg, 1 mg mL^{-1} in PBS); red: human serum albumin (HSA, 5 mg mL^{-1} in PBS); green: fetal bovine serum (FBS, undiluted); blue: undiluted blood plasma (BP, undiluted).

on the gold surface of a SPR sensor chip. Poly(HPMA) brushes were grown using the same procedure as for the silicon substrates to yield 40 nm-thick brushes. The irreversible fouling of human serum albumin (HSA), the main plasma protein, and of fibrinogen (Fbg), a major component of the coagulation cascade, were monitored by SPR. Additionally, the brushes were tested with much more challenging media: undiluted blood plasma (BP) and fetal bovine serum (FBS).

Upon contact of the brushes for 15 min with model solutions of HSA, Fbg and FBS, no fouling could be detected (Fig. 6 and ESI† Table ST4). Only a very minute level of fouling, 18 pg mm^{-2}, could be observed after contact with HBP. This level of fouling represents a decrease in fouling of over 99.5% compared to gold and can be considered negligible. Brushes regarded as having excellent resistance to fouling, such as poly(MeOEGMA) or poly(HOEGMA), typically exhibit a 10-fold higher degree of fouling when challenged with HBP, compared to the present poly(HPMA) system.[69] The excellent resistance of the poly(HPMA) prepared by photoinduced SET-LRP is only comparable with the resistance to fouling provided by non-fouling brushes of carboxybetaine acrylamide (between less than 3 pg mm^{-2} and 100 pg mm^{-2})[36,70] or HPMA (less than 3 pg mm^{-2})[26] prepared by non-living ATRP. The minimum difference among them is less than 0.5% of the fouling on a blank sample. This might be due to variations in the composition of blood plasma of different donors.[71]

Conclusions

The first example of a photoinduced SET-LRP of HPMA is reported. Poly(HPMA) brushes of up to 220 nm were accessible in only 1 h using extremely small amount of copper (80 ppb).

The living nature of this photoinitiated SET-LRP was demonstrated by re-initiation to extend the degree of polymerization of the polymer brush or to form diblock copolymers. The spatial control of the brush growth was demonstrated by the preparation of micropatterns.

The poly(HPMA) brushes combine the unmatched resistance to fouling of previously reported poly(HPMA) brushes with the highly versatile living nature endowed by the photoinduced SET-LRP. Therefore, we anticipate that the new system reported here will lead to a plethora of new applications in the biomaterial and biosensing fields for which an exquisite design of the surface architecture is fundamental to achieve the desired functions.

Experimental

Materials

CuBr$_2$ (99.999% trace metal basis), oligo(ethylene glycol) methyl ether methacrylate (M_n = 300 g mol^{-1}), tris[2-(dimethylamino)ethyl]amine (Me$_6$TREN, 97%), triethylamine (99%), 10-undecen-1-ol (98%), mercaptoundecanol (97%), α-bromoisobutyryl bromide (98%), trichlorosilane (99%), and platinum(0)-1,3-divinyl-1,1,3,3-tetramethyldisiloxane complex solution (Karstedt's catalyst, ~2% Pt in xylene) were obtained from Sigma-Aldrich, Czech Republic and used as received. Extra-dry (over molecular sieves) toluene (99.85%) and dimethyl sulfoxide (99.7%, DMSO) were purchased from Acros, Czech Republic. Ethanol (99.8%), acetone (99.5%), tetrahydrofuran (THF, 99.5%), toluene (99%), and DMSO (99%) were purchased from Lach-Ner, Czech Republic. Deionized water was obtained from a Milli-Q system (Merck-Millipore, Czech Republic). Silicon wafers were purchased from ON Semiconductor, Czech Republic. N-(2-Hydroxypropyl) methacrylamide was synthesized according to literature procedures.[72] Triethylamine was refluxed over CaH$_2$ overnight, distilled, and stored under Ar atmosphere in dark. THF was dried over Na and freshly distilled before use. ω-mercaptoundecyl bromoisobutyrate was synthesized according to a previous report.[73]

Human blood plasma (mix from 5 donors) was provided by the Institute of Hematology and Blood Transfusion, Czech Republic. Fetal bovine serum, fibrinogen and human serum albumin were purchased from Sigma-Aldrich, Czech Republic.

Self-assembled monolayer of initiator

Silicon coupons (~1 × 1 cm^2) were rinsed twice with absolute EtOH and MilliQ water, followed by exposure to air plasma for 20 min to generate hydroxyl groups at the surface able to hydrolyze the chlorides groups of the initiator. The freshly activated surfaces were subsequently immersed in a freshly prepared 1 mg mL^{-1} solution of 11-(trichlorosilyl)undecyl 2-bromo-2-methylpropanoate in dry toluene. The silanization of the substrates to form the self-assembled monolayer was allowed to proceed for 3 h at 25 °C in a dry environment. The substrates were subsequently rinsed with toluene, acetone, EtOH and MilliQ water and blow dried with N$_2$.

For the surface plasmon resonant (SPR) experiment the substrates (chips) were microscope glass slides coated with Ti (a 2.5 nm adhesion layer) and Au (50 nm). The chips were rinsed with ethanol followed by deionized water twice, blow dried with nitrogen and UV-ozone cleaned (Jelight) for 20 min. Subsequently, the substrates were immediately placed in a solution of ω-mercaptoundecyl bromoisobutyrate (1 mM in absolute EtOH) and kept overnight at 25 °C to form the initiator SAM. After rinsing with ethanol and water the samples were blow dried with N_2.

Photoinduced SET-LRP of HPMA

For a typical polymerization experiment in DMSO and at 8.0 ppm of Cu the following procedure was employed: A stock solution (**S**) of $CuBr_2$ (3.9 mM) and Me_6TREN (23.4 mM) was prepared in DMSO. An aliquot of the freshly prepared stock solution **S** (273 μL) was transferred to a round bottomed flask containing DMSO (3.15 mL) to give the solution **A**. In another round bottomed flask, a solution of HPMA (1.55 g, 10.8 mmol) in DMSO (3.00 mL) was prepared (solution **B**). Solutions **A** and **B** were degassed by bubbling Ar for 30 min while stirring and being kept in the dark by wrapping them in Al-foil. Subsequently, solution **A** was transferred using a gas-tight syringe under Ar protection to solution **B** resulting in $[HPMA]_0 = 1.76$ M, $[CuBr_2]_0 = 166$ μM (8.0 ppm), and $[Me_6TREN]_0 = 996$ μM. The combined polymerization solution was stirred and transferred to individual crimped vials containing the initiator-coated Si wafer substrates, which were previously degassed by purging with Ar for 15 min. The polymerization was conducted by irradiating the vials inside a UV-reactor (Salon Edge, Fig. SF1†), consisting of a nail-curing device (four 9 W lamps, $\lambda_{max} = 365$ nm) placed on top of a shaker plate (100 min^{-1}) and kept at room temperature. After irradiation for a preset amount of time, the vials were removed from the reactor, quickly opened and filled with DMSO to quench the polymerization. The samples were removed from the solution and rinsed with DMSO, acetone, absolute ethanol, and water, and dried by blowing with N_2.

For the polymerizations performed in DMSO/water, the same procedure was employed but using a 1 : 1 mixture of DMSO/water instead of pure DMSO ($[HPMA]_0 = 1.76$ M, $[CuBr_2]_0 = 166$ μM (8.0 ppm), and $[Me_6TREN]_0 = 996$ μM). For the polymerizations carried out using 80 ppb of Cu, the same procedure was employed except that the volume of stock catalyst solution **S** added to form **A** was 2.73 μL instead of 273 μL ($[HPMA]_0 = 1.76$ M, $[CuBr_2]_0 = 1.66$ μM (80 ppb), and $[Me_6TREN]_0 = 9.96$ μM).

Chain extension of poly(HPMA)

Poly(HPMA) brushes were grown in DMSO/water (1 : 1) using 80 ppb of Cu ($[HPMA]_0 = 1.76$ M, $[CuBr_2]_0 = 1.66$ μM (80 ppb), and $[Me_6TREN]_0 = 9.96$ μM) as described above. After polymerization for 10 min the substrates were rinsed, dried, and the thickness was measured by ellipsometry (for method, see ESI†). Subsequently, the same substrates were placed in the crimped vials, which were purged for 30 min with Ar before

the addition of freshly degassed polymerization solution using a gas tight syringe. The polymerization was allowed to proceed for 35 min. The samples were removed from the solution and rinsed with DMSO, acetone, absolute ethanol, and water, and dried by blowing with N_2.

Grafting of poly(HPMA-*b*-MeOEGMA)

A first block of poly(HPMA) brushes was prepared by photo-induced SET-LRP of HPMA in DMSO/water using 80 ppb of Cu ($[HPMA]_0 = 1.76$ M, $[CuBr_2]_0 = 1.66$ μM (80 ppb), and $[Me_6TREN]_0 = 9.96$ μM) as described above. The polymerization was allowed to proceed under UV-irradiation for 18 min, after which the samples were rinsed with DMSO, acetone, EtOH (abs) and water, and dried by blowing with N_2.

The second block was prepared by the photoinduced SET-LRP of MeOEGMA. An aliquot of a stock solution **S** (273 μL) of $CuBr_2$ (3.9 mM) and Me_6TREN (23.4 mM) in DMSO was diluted with DMSO (6.15 mL) to give the solution **A** and degassed by Ar bubbling for 30 min in the dark. In a separate round bottomed flask the monomer (MeOEGMA, 3.09 mL, 10.8 mmol) was degassed at 0 °C and was subsequently transferred using a gas-tight syringe under Ar protection to solution **A** resulting in $[MeOEGMA]_0 = 1.76$ M, $[CuBr_2]_0 = 166$ μM, and $[Me_6TREN]_0 = 996$ μM. The polymerization solution was stirred and transferred to individual crimped vials containing the Si substrates with poly(HPMA) brushes used as macroinitiators, which were previously degassed by purging with Ar for 20 min. The polymerization was conducted by irradiating the vials inside a UV-reactor (Salon Edge, 36 W, Fig. SF1 in the ESI†) for 10 min. The vials were removed from the reactor, quickly opened and filled with DMSO to quench the polymerization. The samples were removed from the solution and rinsed with DMSO, acetone, absolute ethanol, and water, and dried by blowing with N_2.

Surface characterization

Spectroscopic ellipsometry. The polymerization kinetics were followed by measuring the dry thickness of the brushes using a J.A. Woollam M-2000X Spectroscopic Ellipsometer. Ellipsometric data were acquired in air at room temperature in the wavelength range $\lambda = 245$–1000 nm at angles of incidence, AOI, of 60, 65, and 70°. The data were fitted with CompleteEASE software using a multilayer model. The thicknesses are reported for 3 points on the surface as mean ± standard deviation. For the thickness mapping by ellipsometry of the photo-patterned samples, data were recorded in the same wavelength range at an AOI of 50° and fitted for each point, on a 1.5 mm × 1.5 mm area covering the region of interest. The sample was scanned in a hexagonal grid (pixel distance 50 μm) employing a motorized translator stage.

Grazing angle attenuated total reflectance Fourier-transform infrared (GAATR-FTIR). The spectra were obtained from the dry polymer layers using a Nicolet Nexus 870 FTIR spectrometer (ThermoFisher Scientific) equipped with a VariGATR attachment (Harrick Scientific Products) under continuous purging with dry air. The polymer-coated surfaces were

pressed on the ATR crystal and spectra were acquired with 256 scans at a resolution of 2 cm^{-1} and processed with OMNIC software.

X-ray photoelectron spectroscopy (XPS). XPS measurements were performed using a K-Alpha+ XPS spectrometer (Thermo-Fisher Scientific, UK). The data acquisition and processing using the Thermo Avantage software is described elsewhere.[74] All samples were analyzed using a microfocused, monochromated Al Kα X-ray source (400 μm spot size). The K-Alpha charge compensation system was employed during analysis, using electrons of 8 eV energy, and low-energy argon ions to prevent any localized charge build-up. The XPS depth profiling was performed utilizing the MAGCIS source operated in small cluster ion mode at 8000 eV. Each sputtering cycle lasted 10 s and an area of 2 mm × 1 mm was rastered. The etching rate was determined to be 0.07 nm s^{-1}. XPS spectra acquired in between etch cycles allowed quantitative determination of the moieties present in the block-copolymer layer.

The spectra were fitted with one or more Voigt profiles (binding energy uncertainty: ±0.2 eV) The analyzer transmission function, Scofield sensitivity factors,[75] and effective attenuation lengths (EALs) for photoelectrons were applied for quantification. EALs were calculated using the standard TPP-2M formalism.[76] All spectra were referenced to the C 1s peak attributed to C–C, C–H at 285.0 eV binding energy, which were controlled by means of the well-known photoelectron peaks of metallic Cu, Ag, and Au.

Dynamic water contact angle. The wettability of the surfaces was assessed by the dynamic water contact angle using the sessile drop method with a DataPhysics *OCA 20* instrument. A 5 μL drop was deposited on the surface and its volume was increased up to 15 μL and decreased back to 5 μL at a flow rate of 0.5 μL s^{-1}. The drop profile was recorded during the process and was fitted with a circular algorithm, from which the advancing and receding contact angles were extracted.

Atomic force microscopy (AFM). AFM Images were acquired with a Multimode Atomic Force Microscope NanoScope IIIa (Digital Instruments) as topographical scans in tapping mode in air, using silicon probes OTESPA-R3 (Bruker) with a nominal spring constant of 26 N m^{-1} and a tip radius of 7 nm. Areas of 5 × 5 μm^2 (512 × 512 pixels) were scanned at a rate of 1 Hz. The scans were analyzed using Gwyddion software.

Stylus profilometry. Stylus profilometry was performed using Tencor P-10 Surface Profiler (Texas, USA). Topography scans over areas of 600 × 700 μm^2 were acquired at a speed of 20 μm s^{-1} and sampling rate of 100 Hz. The stylus force was set at 0.01 N.

Surface plasmon resonance. A custom-built SPR instrument (Institute of Photonics and Electronics, Academy of Sciences of the Czech Republic, Prague) based on the Kretschmann geometry of the attenuated total reflection method and spectral interrogation of the SPR conditions was used. The tested solutions of proteins or bodily fluids were driven by a peristaltic pump through four independent channels of a flow cell, in which the SPR responses were simultaneously measured as shifts in the resonant wavelength, λ_{res}. The sensor response ($\Delta\lambda_{res}$) was obtained as the difference between the baselines in phosphate buffered saline (PBS) before and after the injection of the tested samples: human blood plasma, fetal bovine serum, human serum albumin and fibrinogen. The sensor response was calibrated to the mass deposited at the surface of bound molecules. According to a calibration made by Fourier-transform infrared grazing angle specular reflectance, a shift $\Delta\lambda_{res} = 1$ nm corresponds to a change in the deposited protein mass of 150 pg mm^{-2}.[21]

Acknowledgements

Notes and references

1 D. F. Williams, *Biomaterials*, 2009, **30**, 5897–5909.
2 C. Blaszykowski, S. Sheikh and M. Thompson, *Chem. Soc. Rev.*, 2012, **41**, 5599–5612.
3 A. Hucknall, S. Rangarajan and A. Chilkoti, *Adv. Mater.*, 2009, **21**, 2441–2446.
4 S. Jiang and Z. Cao, *Adv. Mater.*, 2010, **22**, 920–932.
5 C. Rodriguez Emmenegger, E. Brynda, T. Riedel, Z. Sedlakova, M. Houska and A. B. Alles, *Langmuir*, 2009, **25**, 6328–6333.
6 Q. Yu, Y. Zhang, H. Wang, J. Brash and H. Chen, *Acta Biomater.*, 2011, **7**, 1550–1557.
7 D. Rana and T. Matsuura, *Chem. Rev.*, 2010, **110**, 2448–2471.
8 J. Homola, *Chem. Rev.*, 2008, **108**, 462–493.
9 C. Rodriguez-Emmenegger, A. Jäger, E. Jäger, P. Stepanek, A. B. Alles, S. S. Guterres, A. R. Pohlmann and E. Brynda, *Colloids Surf., B*, 2011, **83**, 376–381.
10 A. Verma and F. Stellacci, *Small*, 2010, **6**, 12–21.
11 I. Lynch, T. Cedervall, M. Lundqvist, C. Cabaleiro-Lago, S. Linse and K. A. Dawson, *Adv. Colloid Interface Sci.*, 2007, **134–135**, 167–174.
12 M. Lundqvist, J. Stigler, G. Elia, I. Lynch, T. Cedervall and K. A. Dawson, *Proc. Natl. Acad. Sci. U. S. A.*, 2008, **105**, 14265–14270.
13 I. Lynch and K. A. Dawson, *Nano Today*, 2008, **3**, 40–47.
14 K. Knop, R. Hoogenboom, D. Fischer and U. S. Schubert, *Angew. Chem., Int. Ed.*, 2010, **49**, 6288–6308.

15 H. Thissen, T. Gengenbach, R. du Toit, D. F. Sweeney, P. Kingshott, H. J. Griesser and L. Meagher, *Biomaterials*, 2010, **31**, 5510–5519.

16 B. D. Ratner, *Biomaterials*, 2007, **28**, 5144–5147.

17 C. Blaszykowski, S. Sheikh and M. Thompson, *Trends Biotechnol.*, 2014, **32**, 61–62.

18 V. Erwin A, *Biomaterials*, 2012, **33**, 1201–1237.

19 L. Y. Li, S. F. Chen and S. Y. Jiang, *J. Biomater. Sci., Polym. Ed.*, 2007, **18**, 1415–1427.

20 C. Rodriguez-Emmenegger, M. Houska, A. B. Alles and E. Brynda, *Macromol. Biosci.*, 2012, **12**, 1413–1422.

21 C. Rodriguez-Emmenegger, E. Brynda, T. Riedel, Z. Sedlakova, M. Houska and A. B. Alles, *Langmuir*, 2009, **25**, 6328–6333.

22 C. Zhao, L. Li and J. Zheng, *Langmuir*, 2010, **26**, 17375–17382.

23 Q. Shao and S. Jiang, *Adv. Mater.*, 2015, **27**, 15–26.

24 A. L. Lewis, *Colloids Surf., B*, 2000, **18**, 261–275.

25 Z. Zhang, S. Chen and S. Jiang, *Biomacromolecules*, 2006, **7**, 3311–3315.

26 C. Rodriguez-Emmenegger, E. Brynda, T. Riedel, M. Houska, V. Šubr, A. Bologna Alles, E. Hasan, J. E. Gautrot and W. T. S. Huck, *Macromol. Rapid Commun.*, 2011, **32**, 952–957.

27 J. Kopecek and H. Bazilová, *Eur. Polym. J.*, 1973, **9**, 7–14.

28 K. Wu, J. Liu, R. Johnson, J. Yang and J. Kopeček, *Angew. Chem., Int. Ed.*, 2010, **122**, 1493–1497.

29 J. Kopecek and P. Kopecková, *Adv. Drug Delivery Rev.*, 2010, **62**, 122–149.

30 R. Duncan and M. J. Vicent, *Adv. Drug Delivery Rev.*, 2010, **62**, 272–282.

31 E. Jager, A. Jager, T. Etrych, F. C. Giacomelli, P. Chytil, A. Jigounov, J.-L. Putaux, B. Rihova, K. Ulbrich and P. Stepanek, *Soft Matter*, 2012, **8**, 9563–9575.

32 F. Surman, T. Riedel, M. Bruns, N. Y. Kostina, Z. Sedláková and C. Rodriguez-Emmenegger, *Macromol. Biosci.*, 2015, DOI: 10.1002/mabi.201400470.

33 J. T. Rademacher, M. Baum, M. E. Pallack, W. J. Brittain and W. J. Simonsick, *Macromolecules*, 2000, **33**, 284–288.

34 C. Konák, B. Ganchev, M. Teodorescu, K. Matyjaszewski, P. Kopecková and J. Kopecek, *Polymer*, 2002, **43**, 3735–3741.

35 M. Teodorescu and K. Matyjaszewski, *Macromolecules*, 1999, **32**, 4826–4831.

36 H. Vaisocherova, V. Sevcu, P. Adam, B. Spackova, K. Hegnerova, A. de los Santos Pereira, C. Rodriguez-Emmenegger, T. Riedel, M. Houska, E. Brynda and J. Homola, *Biosens. Bioelectron.*, 2014, **51**, 150–157.

37 Y. Li, M. Giesbers, M. Gerth and H. Zuilhof, *Langmuir*, 2012, **28**, 12509–12517.

38 V. Šubr, L. Kostka, J. Strohalm, T. Etrych and K. Ulbrich, *Macromolecules*, 2013, **46**, 2100–2108.

39 C. Rodriguez-Emmenegger, B. V. Schmidt, Z. Sedlakova, V. Subr, A. B. Alles, E. Brynda and C. Barner-Kowollik, *Macromol. Rapid Commun.*, 2011, **32**, 958–965.

40 M. Zamfir, C. Rodriguez-Emmenegger, S. Bauer, L. Barner, A. Rosenhahn and C. Barner-Kowollik, *J. Mater. Chem. B*, 2013, **1**, 6027–6034.

41 R. C. Advincula, W. J. Brittain, K. C. Caster and R. Jürgen, *Polymer Brushes: Synthesis, Characterization, Applications*, Wiley Interscience, 2004.

42 V. Percec, A. V. Popov, E. Ramirez-Castillo and O. Weichold, *J. Polym. Sci., Part A: Polym. Chem.*, 2003, **41**, 3283–3299.

43 V. Percec, A. V. Popov, E. Ramirez-Castillo, M. Monteiro, B. Barboiu, O. Weichold, A. D. Asandei and C. M. Mitchell, *J. Am. Chem. Soc.*, 2002, **124**, 4940–4941.

44 B. M. Rosen and V. Percec, *Chem. Rev.*, 2009, **109**, 5069–5119.

45 N. Zhang, S. R. Samanta, B. M. Rosen and V. Percec, *Chem. Rev.*, 2014, **114**, 5848–5958.

46 V. Percec, T. Guliashvili, J. S. Ladislaw, A. Wistrand, A. Stjerndahl, M. J. Sienkowska, M. J. Monteiro and S. Sahoo, *J. Am. Chem. Soc.*, 2006, **128**, 14156–14165.

47 N. H. Nguyen, M. E. Levere and V. Percec, *J. Polym. Sci., Part A: Polym. Chem.*, 2012, **50**, 860–873.

48 N. H. Nguyen, M. E. Levere, J. Kulis, M. J. Monteiro and V. Percec, *Macromolecules*, 2012, **45**, 4606–4622.

49 G. Lligadas and V. Percec, *J. Polym. Sci., Part A: Polym. Chem.*, 2007, **45**, 4684–4695.

50 N. H. Nguyen, J. Kulis, H.-J. Sun, Z. Jia, B. van Beusekom, M. E. Levere, D. A. Wilson, M. J. Monteiro and V. Percec, *Polym. Chem.*, 2013, **4**, 144–155.

51 S. R. Samanta, R. Cai and V. Percec, *Polym. Chem.*, 2014, **5**, 5479–5491.

52 N. H. Nguyen, C. Rodriguez-Emmenegger, E. Brynda, Z. Sedlakova and V. Percec, *Polym. Chem.*, 2013, **4**, 2424–2427.

53 S. R. Samanta, V. Nikolaou, S. Keller, M. J. Monteiro, D. A. Wilson, D. M. Haddleton and V. Percec, *Polym. Chem.*, 2015, **6**, 2084–2097.

54 X. A. Jiang, B. M. Rosen and V. Percec, *J. Polym. Sci., Part A: Polym. Chem.*, 2010, **48**, 2716–2721.

55 X. Jiang, B. M. Rosen and V. Percec, *J. Polym. Sci., Part A: Polym. Chem.*, 2010, **48**, 2716–2721.

56 N. H. Nguyen and V. Percec, *J. Polym. Sci., Part A: Polym. Chem.*, 2011, **49**, 4756–4765.

57 A. H. Soeriyadi, C. Boyer, F. Nyström, P. B. Zetterlund and M. R. Whittaker, *J. Am. Chem. Soc.*, 2011, **133**, 11128–11131.

58 M. Teodorescu and K. Matyjaszewski, *Macromol. Rapid Commun.*, 2000, **21**, 190–194.

59 A. Anastasaki, V. Nikolaou, Q. Zhang, J. Burns, S. R. Samanta, C. Waldron, A. J. Haddleton, R. McHale, D. Fox, V. Percec, P. Wilson and D. M. Haddleton, *J. Am. Chem. Soc.*, 2014, **136**, 1141–1149.

60 E. Larsson, S. A. Pendergraph, T. Kaldeus, E. Malmstrom and A. Carlmark, *Polym. Chem.*, 2015, **6**, 1865–1874.

61 S. Tugulu and H.-A. Klok, *Biomacromolecules*, 2008, **9**, 906–912.

62 D. Paripovic and H. A. Klok, *Macromol. Chem. Phys.*, 2011, **212**, 950–958.

63 V. V. Naik, R. Städler and N. D. Spencer, *Langmuir*, 2014, **30**, 14824–14831.

64 E. A. Vogler, J. C. Graper, G. R. Harper, H. W. Sugg, L. M. Lander and W. J. Brittain, *J. Biomed. Mater. Res.*, 1995, **29**, 1005–1016.

65 W. Norde and J. Lyklema, *J. Colloid Interface Sci.*, 1979, **71**, 350–366.

66 X. Jiang, J. Wu, L. Zhang, Z. Cheng and X. Zhu, *Macromol. Rapid Commun.*, 2014, **35**, 1879–1885.

67 A. Anastasaki, V. Nikolaou, N. W. McCaul, A. Simula, J. Godfrey, C. Waldron, P. Wilson, K. Kempe and D. M. Haddleton, *Macromolecules*, 2015, **48**, 1404–1411.

68 J. Trmcic-Cvitas, E. Hasan, M. Ramstedt, X. Li, M. A. Cooper, C. Abell, W. T. S. Huck and J. E. Gautrot, *Biomacromolecules*, 2009, **10**, 2885–2894.

69 T. Riedel, Z. Riedelova-Reicheltova, P. Majek, C. Rodriguez-Emmenegger, M. Houska, J. E. Dyr and E. Brynda, *Langmuir*, 2013, **29**, 3388–3397.

70 H. Vaisocherova, Z. Zhang, W. Yang, Z. Q. Cao, G. Cheng, A. D. Taylor, M. Piliarik, J. Homola and S. Y. Jiang, *Biosens. Bioelectron.*, 2009, **24**, 1924–1930.

71 A. de los Santos Pereira, C. Rodriguez-Emmenegger, F. Surman, T. Riedel, A. Bologna and E. Brynda, *RSC Adv.*, 2014, **4**, 2318–2321.

72 K. Ulbrich, V. Subr, J. Strohalm, D. Plocova, M. Jelinkova and B. Rihova, *J. Controlled Release*, 2000, **64**, 63–79.

73 D. M. Jones, A. A. Brown and W. T. S. Huck, *Langmuir*, 2002, **18**, 1265–1269.

74 K. L. Parry, A. G. Shard, R. D. Short, R. G. White, J. D. Whittle and A. Wright, *Surf. Interface Anal.*, 2006, **38**, 1497–1504.

75 J. H. Scofield, *J. Electron. Spectrosc. Relat. Phenom.*, 1976, **8**, 129–137.

76 S. Tanuma, C. J. Powell and D. R. Penn, *Surf. Interface Anal.*, 1993, **21**, 165–176.